

# Revisiting the OH-CH correlation in diffuse clouds

Bhaswati Mookerjee<sup>\*</sup>

<sup>1</sup>Tata Institute of Fundamental Research, Homi Bhabha Road, Mumbai 400005, India

Accepted 2016 April 12. Received 2016 April 08; in original form 2016 February 26

## ABSTRACT

Based on the analysis of available published data and archival data along 24 sightlines (5 of which are new) we derive more accurate estimates of the column densities of OH and CH towards diffuse/translucent clouds and revisit the typically observed correlation between the abundances of these species. The increase in the sample size was possible because of the equivalence of the column densities of CH derived from a combination of the transitions at 3137 & 3143, and a combination of transitions at 3886 & 3890, which we have demonstrated here. We find that with the exception of four diffuse clouds, the entire source sample shows a clear correlation between the column densities of OH and CH similar to previous observations. The analysis presented also verifies the theoretically predicted oscillator strengths of the OH A–X (3078 & 3082), CH B–X (3886 & 3890) and C–X (3137 & 3143) transitions. We estimate  $N(\text{H})$  and  $N(\text{H}_2)$  from the observed  $E(B - V)$  and  $N(\text{CH})$  respectively. The  $N(\text{OH})/N(\text{CH})$  ratio is not correlated with the molecular fraction of hydrogen in the diffuse/translucent clouds. We show that with the exception of HD 34078 for all the clouds the observed column density ratios of CH and OH can be reproduced by simple chemical models which include gas-grain interaction and gas-phase chemistry. The enhanced  $N(\text{OH})/N(\text{CH})$  ratio seen towards the 3 new sightlines can be reproduced primarily by considering different cosmic ray ionization rates.

**Key words:** ISM: molecules — Astrochemistry

## 1 INTRODUCTION

The OH molecule was discovered using the  $\Lambda$  doublet transition observed between the levels of the ground rotational state  $^2\Pi_{3/2}$   $J = 3/2$  at 18 cm (Weinreb et al. 1963); later its electronic transitions were identified in ultraviolet spectra of bright OB-stars (Crutcher & Watson 1976; Chaffee & Lutz 1977; Felenbok & Roueff 1996). Two lines of the  $A^2\Sigma^+ - X^2\Pi_i$  band near 3078 and 3082 are available to ground-based observatories and in a series of papers (Weselak et al. 2009, 2010) estimates of OH column densities along 17 translucent lines of sight from these transitions have been derived. These observations performed using the high-resolution VLT/UVES-spectrograph verified the oscillator strengths for the 3078 and 3082 and also suggested a close correlation between the column densities of OH and CH molecules. Early chemical models have suggested production of hydrides like OH and NH due to grain catalysis reactions (Wagenblast et al. 1993). Hence observation of OH to derive abundances towards translucent sightlines with larger than normal far-UV extinction is interesting. In-

terstellar CH is often observed using its strongest A–X transition at 4300. However this line being saturated, reliable estimates of CH column densities are derived from the spectral lines due to the weaker B–X system at 3886 (Krelowski et al. 1999; Weselak et al. 2004). There exist many studies of CH to explore its correlation to the diffuse interstellar bands (DIBs) at 5780 and 5797 (Krelowski et al. 1999). However availability of data for OH is significantly worse. Observations have shown the abundances of CH molecule to be tightly correlated with those of the  $\text{H}_2$  molecule (Mattila 1986; Weselak et al. 2004; Sheffer et al. 2008). The correlation is sufficiently strong so that in many recent studies column densities of CH have been used to derive estimates for  $\text{H}_2$  column density (Sheffer et al. 2008; Wiesemeyer et al. 2016). The correlation is understood in terms of higher formation rates of CH in reactions involving molecular hydrogen.

The aim of this work is to incorporate the newly available OH and CH data for 13 lines of sight (5 of which are new) in order to investigate the correlation between OH and CH in diffuse/translucent molecular clouds. This correlation is particularly interesting considering the tight correlation between CH and  $\text{H}_2$ . We shall show that the oscillator

<sup>\*</sup> E-mail: bhaswati@tifr.res.in

strengths for the C–X system of lines of CH at 3137 are correct so that these can be equivalently used to determine the column densities of CH. We shall use simple chemical models to check whether the observed correlation between OH and CH or the absence of it is predicted by the chemical models.

## 2 UV SPECTROSCOPIC DATASETS

We extend the analysed sample of [Weselak et al. \(2010\)](#) by combining it with sample of the highly reddened early-type stars which were analyzed by [Bhatt & Cami \(2015\)](#). In order to complete the information on all the lines of sight as much as possible, we have also analyzed fully processed UVES/VLT data of both pairs of CH lines, obtained from the ESO Science Archive Facility<sup>1</sup>. [Bhatt & Cami \(2015\)](#) had identified 30 known features (11 atomic and 19 molecular) and tentatively detected up to 7 new interstellar absorption lines of unknown origin towards 346 targets. Out of this entire sample only for 13 sources observations of both the 3078 and 3082 transitions of OH were available. Out of these 13 sources 8 were already present in the sample used by [Weselak et al. \(2010\)](#). The observed data for the two CH transitions  $B^2\Sigma^- - X^2\Pi_i$  at 3886 and 3890 for 19 of these sightlines were also presented by [Weselak et al. \(2010\)](#). [Bhatt & Cami \(2015\)](#) presented the  $C^2\Sigma^+ - X^2\Pi_i$  transitions of CH at 3137 and 3143 for the 12 out of the 13 sources in which OH was observed. Thus we finally have 24 sources, 19 from [Weselak et al. \(2010\)](#) and 13 from [Bhatt & Cami \(2015\)](#), of which 5 sightlines are new.

## 3 RESULTS AND DISCUSSION

Table 1 presents the spectroscopic details, frequencies, and  $f$ -values of the transitions of OH and CH considered here.

Table 2 presents the observed equivalent widths (EW) of the OH lines at 3078 and 3082 and Fig. 1 shows a plot of the same. We find that excluding HD 114213 (with the largest EW(3082)), the equivalent widths of the two transitions show a correlation of 0.92, which is somewhat worse than the estimates of [Weselak et al. \(2009\)](#). From the slope of the line of regression we estimate the ratio of the equivalent widths of the two transitions to be  $1.62 \pm 0.08$ . The wavelengths of the two transitions being similar, the equivalent widths are expected to have a ratio similar to the ratio of the  $f$ -values of the two transitions. The derived ratio matches well with the estimate (1.62) based on the  $f$ -values of the two transitions.

For all the unsaturated lines of OH and CH we estimate the column densities using the relationship proposed by [Herbig \(1968\)](#):

$$N = 1.13 \times 10^{20} W_\lambda / (\lambda^2 f) \quad (1)$$

where  $W_\lambda$  and  $\lambda$  are in  $\text{\AA}$ , column density is in  $\text{cm}^{-2}$  and the  $f$ -values used are taken from Table 1. The total column density for OH is estimated by adding the column densities of the 3078 and 3082 transitions (Table 2).

<sup>1</sup> <http://www.eso.org/sci/observing/phase3.html>

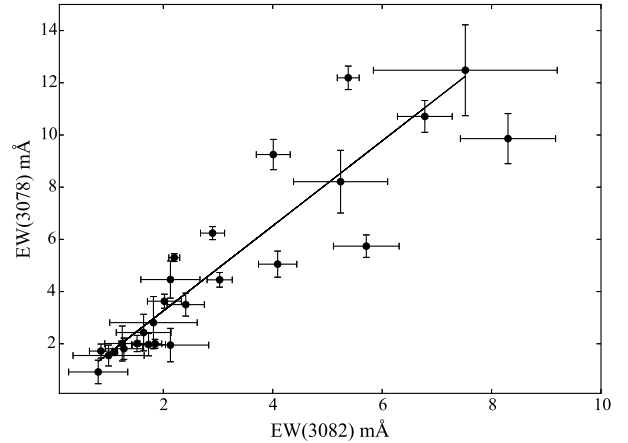


**Figure 1.** Comparison of the equivalent widths of the two transitions of OH at 3078 and 3082. The straight line corresponds to a linear regression with a correlation coefficient of 0.92 and a slope of  $1.62 \pm 0.08$ .

Out of the 24 sources, for 19 sources we have measurements of the 3137 and 3143 transitions and for 22 sources we have measurements of the 3886 and 3890 transitions of CH (Table 2). We have re-measured all the CH equivalent widths from the UVES/VLT archival data and find that in most cases our measurements are consistent with the published work of [Weselak et al. \(2010\)](#); [Bhatt & Cami \(2015\)](#). We have revised the values of the equivalent width of the 3886 CH line towards HD 27778 and both the 3886 and the 3890 CH lines towards HD 154445. Figure 2 shows a comparison of CH column densities derived from a combination of the transitions at 3137 & 3143 with  $N(\text{CH})$  derived from a combination of transitions at 3886 & 3890 for the 17 sources in which both sets of CH lines have been observed. The values of  $N(\text{CH})$  show a correlation of 0.99 with  $N(\text{CH}(3137+3143))/N(3886+3890) = 1.03 \pm 0.02$ . For the rest of the analysis, we thus use the column densities for the pair of CH transitions which shows a lower relative uncertainty.

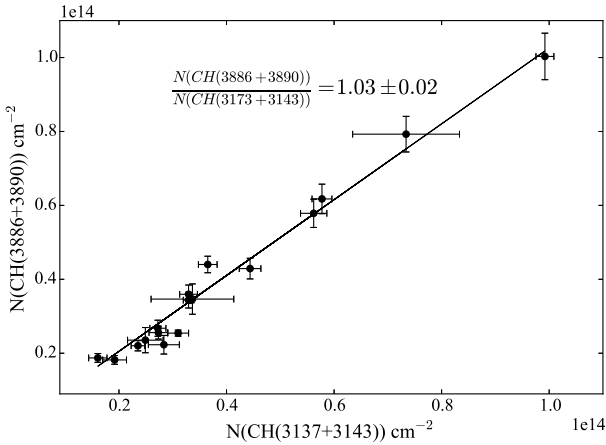
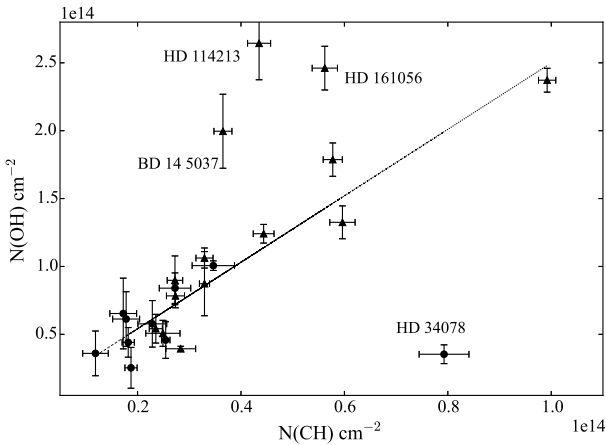
Figure 3 shows a plot of estimated  $N(\text{OH})$  as a function of  $N(\text{CH})$ . For clarity, we have used different symbols to indicate which of the two pairs of transitions was used to derive the  $N(\text{CH})$ . We find that for most of the sightlines the column densities of OH and CH occupy a band in the plot, except towards BD-14 5037, HD 114213, HD 161056 and HD 34078. The overall correlation coefficient is 0.61 between  $N(\text{OH})$  and  $N(\text{CH})$ , which is significantly worse than the value presented by [Weselak et al. \(2009\)](#). However, the correlation coefficient improves to 0.94 (black dashed line) when the four outliers are removed, although it is still less than the 0.99 obtained by [Weselak et al. \(2010\)](#). For the 4 out of 24 sightlines which do not show the correlation between  $N(\text{OH})$  and  $N(\text{CH})$  as seen in the other source, the deviation can not be explained in terms of the observational uncertainties.

Combined analysis of all available datasets on OH and CH observations of diffuse clouds enable us to further revise the relation between the column densities of the two molecules for 20 sightlines to  $[N(\text{OH}) = 2.41 \pm 0.21 N(\text{CH})$

**Table 1.** Spectroscopic details and  $f$ -values of OH and CH transitions studied. CH transitions

Species	Vibronic Band	Rotational lines	Position	Ref.	$f$ -value	Ref.
OH	$A^2\Sigma^+-X^2\Pi_i$ (0,0)	$Q_1(3/2)+^Q P_{21}(3/2)$	3078.443	1	0.00105	2
		$P_1(3/2)$	3081.6643	1	0.000648	2
CH	$C^2\Sigma^+-X^2\Pi_i$ (0,0)	$R_2$	3137.576	3	0.00210	3
		$Q_2(1)+^Q R_{12}(1)$	3143.150	3	0.00640	3
CH	$B^2\Sigma^--X^2\Pi_i$ (0,0)	$Q_2(1)+^Q R_{12}(1)$	3886.409	3	0.00320	3
		$^P Q_{12}(1)$	3890.217	3	0.00210	3

1. Weselak et al. (2009), 2. Felenbok & Roeff (1996) and 3. Lien (1984)

**Figure 2.** Comparison of  $N(\text{CH})$  derived for the 17 sources in which both pairs of transitions *viz.*, (3137 & 3143) and (3886 & 3890) are available. The straight line shown is fitted to obtain the ratio between the two column densities.**Figure 3.** Variation of  $N(\text{OH})$  as a function of  $N(\text{CH})$ . Filled circles and triangles denote  $N(\text{CH})$  derived from the (3137+3143) and (3886+3890) transitions, respectively. Black dashed line shows the linear fit to all datapoints excluding the outliers HD 34078, HD 114213, HD 161056 and BD-14 5037, which corresponds to a Pearson correlation coefficient of 0.94.

$+(8.55 \pm 7.17)$  (in  $10^{12} \text{ cm}^{-2}$ ). The relationship derived by Weselak et al. (2010) had made use of 16 sightlines. The ratio of column densities of OH and CH is found to vary between 1.5 to 4.1 in diffuse clouds.

We look into the 3 sources HD 114213, HD 161056 and BD-14 5037 for possible observational reasons behind the very different  $N(\text{CH})$ - $N(\text{OH})$  relationship, based on the central heliocentric velocities of the absorption features. The source BD-14 5037 shows absorptions at two velocities around  $-6 \text{ km s}^{-1}$  and  $6 \text{ km s}^{-1}$ . Since only  $-6 \text{ km s}^{-1}$  component is seen in the OH(3081) spectral line, the numbers we have used correspond to this component. Similarly, the line of sight toward HD 114213 shows absorptions at two velocities: CH lines show up at  $-16$  and  $6 \text{ km s}^{-1}$ , while the OH 3078 line is at  $-17 \text{ km s}^{-1}$  and  $3 \text{ km s}^{-1}$  while the OH(3082) line is at  $-20 \text{ km s}^{-1}$  and  $0.3 \text{ km s}^{-1}$ . We have used here the  $-20 \text{ km s}^{-1}$ , which is identified in all the spectral lines considered here, since the relative shift in the velocity is smaller than the observed FWHM of the lines (Bhatt & Cami 2015). The sightline towards HD 161056 however shows only one velocity component, although the heliocentric velocities at 3078, 3082, 3137 and 3146 are  $-9.4 \pm 0.1$ ,  $-11.0 \pm 0.1$ ,  $-12.7 \pm 0.3$  and  $-14.0 \pm 0.3 \text{ km s}^{-1}$  respectively (Bhatt & Cami 2015). As with the other two sources, the shifts in central velocities are smaller than the FWHM of the lines. Thus, for the three sources HD 114213, HD 161056 and BD-14 5037 as with HD 34078 the lack of correlation between  $N(\text{CH})$  and  $N(\text{OH})$  can not be explained in terms of any observational uncertainties. It is clearly obvious that along the sightlines towards HD 114213, HD 161056 and BD-14 5037, the OH/CH ratio are 2–3 times the value seen in the other diffuse clouds.

#### 4 MOLECULAR HYDROGEN FRACTION IN DIFFUSE CLOUDS

Based on theoretical predictions and the observed correlations between CH and  $\text{H}_2$ , of late  $N(\text{H}_2)$  is often derived from the observed  $N(\text{CH})$  assuming  $\text{CH}/\text{H}_2 = 3.5 \times 10^{-8}$  (Sheffer et al. 2008; Wiesemeyer et al. 2016, and references therein). It is also possible to estimate the column density of hydrogen nuclei using the measured  $E(B - V)$  by using the relationship  $N(\text{H}) = 5.8 \times 10^{21} E(B - V)$  (Bohlin, Savage, & Drake 1978). For all the lines of sight considered here, since both  $E(B - V)$  and  $N(\text{CH})$  are available, we have estimated  $f_{\text{H}_2} = \frac{N(\text{H}_2)}{N(\text{H})}$  and do not find any correlation between  $N(\text{CH})/N(\text{OH})$  and  $f_{\text{H}_2}$ . The sources, HD 161056 and HD 114213, both of which show high

$N(\text{OH})/N(\text{CH})$  ratios have  $f_{\text{H}_2}$  of 51% and 19% respectively. For 17 lines of sight  $f_{\text{H}_2}$  is  $\leq 0.4$ , with BD-14 5037 and HD 34078 showing 11% and 80% molecular hydrogen fraction, respectively. We discuss the anomalously high  $N(\text{CH})$  shown by HD 34078 later in the paper.

## 5 CHEMICAL MODELING OF THE DIFFUSE CLOUDS

We have constructed chemical models for the diffuse/translucent clouds using the Astrochem code (Maret & Bergin 2015) together with the reaction coefficients from the OSU 2009 and examined the predicted OH and CH abundances. The models consider a variety of gas phase processes, as well as simple gas-grain interactions, such as the freeze-out and desorption via several mechanisms (thermal desorption, cosmic-ray desorption and photo-desorption). We have run a grid of models covering a range of values for the relevant physical parameters in order to ascertain the parameters to which the CH and OH abundances are the most sensitive. We used the abundances of both CH and OH at  $10^6$  yr since both attain a constant value beyond  $10^5$  yr. Typically in these models, OH abundances are quite sensitive to the cosmic ray ionization rate ( $\zeta_{\text{CR}}$ ), with the abundance decreasing with increase in  $\zeta_{\text{CR}}$ . Figure 4 shows a plot of  $N(\text{OH})$  as a function of  $N(\text{CH})$  as predicted by the models which are detailed in the caption. The purpose of constructing these models is to understand whether these also predict the observed correlation between  $N(\text{CH})$  and  $N(\text{OH})$  and not to model the diffuse/translucent clouds each line of sight accurately. The modeling is also aimed to understand whether the four lines of sight which lie outside of the correlation band (Fig. 3) are generally consistent with these simple chemical models that consider gas-grain interactions and gas-phase reactions but do not include the effects of shock or turbulence.

We have considered multiple values of  $N(\text{CH})$  and used the CH abundances predicted by a model corresponding to a set of input parameters to estimate  $N(\text{H}_2)$  and then used this  $N(\text{H}_2)$  to estimate  $N(\text{OH})$  from the OH abundances predicted by the model. In Fig. 4 we plot the observed values of  $N(\text{OH})$  and  $N(\text{CH})$  for the 24 sightlines presented here. We find that broadly the model corresponding to  $n_{\text{H}}=500 \text{ cm}^{-3}$ ,  $\zeta_{\text{CR}} = 10^{-14} \text{ s}^{-1}$ ,  $A_{\text{V}}=2.0$ ,  $f_{\text{H}_2}=0.3$ , UV radiation ( $\chi$ ) = 5 and  $T_{\text{gas}}=30 \text{ K}$  (solid black line in Fig. 4) is consistent with many of the observed CH and OH column densities and we designate this as Model A in the remaining discussion. For all models discussed here the following initial abundances relative to H were assumed  $[\text{He}]=0.14$ ,  $[\text{N}]=2.14 \times 10^{-5}$ ,  $[\text{O}]=1.76 \times 10^{-4}$ ,  $[\text{C}^+]=7.3 \times 10^{-5}$  and  $[\text{e}^+]=7.3 \times 10^{-5}$ .

In order to estimate the effect of variation in the input parameters we also show predictions from models in which the parameters like  $n_{\text{H}}$ ,  $\zeta_{\text{CR}}$  and  $A_{\text{V}}$  are varied relative to the parameters of Model A, one parameter at a time (Fig. 4). Relative to Model A, the presence of correlation between OH and CH does not change drastically when a)  $f_{\text{H}_2}$  is varied up to 0.8, b)  $T_{\text{gas}}$  is assumed to be 10 and 20 K and c)  $\chi$  is reduced to 1. In order to show that it is indeed possible to find a chemical model which is reasonably consistent with ob-

served parameters and still reproduce the observed OH/CH ratio for one of the outliers we have constructed a model for HD 114213, one of the outliers. Shown in left bottom panel of Fig. 4 in green continuous line is the prediction of a model with  $A_{\text{V}}=3.0$  (consistent with observed  $E(B-V)$ ),  $n_{\text{H}}=500 \text{ cm}^{-3}$ ,  $\zeta_{\text{CR}}=2.5 \times 10^{-16} \text{ s}^{-1}$ ,  $T_{\text{gas}}=30 \text{ K}$  and  $f_{\text{H}_2}=0.3$ , which reproduces the observed  $N(\text{OH})$  and  $N(\text{CH})$  quite well. This is by no means a unique model, since there are several free parameters and fewer observational constraints, however this shows that the observed column density ratios are not inconsistent with the chemical models. Thus overall, we find that with the exception of HD 34078, the observed ratio of column densities of OH and CH can be reproduced in all clouds by the chemical models which do not involve any shock chemistry. The extremely low  $N(\text{OH})$  relative to  $N(\text{CH})$  as seen in HD 34078 can not be explained even by varying the input parameters over a much larger range than what has been shown in Fig. 4.

The line of sight towards HD 34078 has been studied extensively using FUSE spectra and later millimeter CO observations by Boissé et al. (2005, 2009). This line of sight shows anomalously high CH/H<sub>2</sub> as well as CH<sup>+</sup>/H<sub>2</sub> ratios which have been explained by the presence of a nascent bow shock around the star, at the interface between the stellar wind and the ambient interstellar medium, where the material is strongly compressed (Boissé et al. 2005). There is no corresponding enhancement of OH abundance, which indicates that the OH absorption is due to the more quiescent H<sub>2</sub> gas located beyond the photodissociation front and shocked region (Boissé et al. 2009).

The correlation of CH with H<sub>2</sub> is explained in terms of the higher formation rates of CH due to reactions involving molecular hydrogen (Federman 1982). The formation of OH on the other hand is strongly influenced by grain-surface catalysis, which implies that presence of dust grains (and hence possibly H<sub>2</sub>) would enhance OH formation rates (Wagenblast et al. 1993). This can be a possible reason behind the significant correlation between OH and CH in translucent clouds. However as seen from the chemical models several combinations of the input parameters can lead to similar abundance ratios for the two species. Thus in order to obtain a more quantitative view of the correlation, accurate modeling of individual sources with further constraining observations is necessary.

## 6 CONCLUSIONS

The equivalence of the CH column densities derived from a combination of transitions at 3137 and 3143 and a combination of transitions at 3886 and 3890 has enabled us to combine types of CH datasets. This has resulted in an increase in the number of sightlines for which both  $N(\text{OH})$  and  $N(\text{CH})$  have been observed. With the exception of four sightlines, the column density of OH appears to correlate well with the CH column density in all sources. The derived relationship between  $N(\text{OH})$  and  $N(\text{CH})$  is thus based on a dataset with larger number of sightlines observed with lower uncertainties than the previous determinations. These results also verify the oscillator strengths for all the transitions which have been observed. We find that the  $N(\text{OH})/N(\text{CH})$  ratio is not correlated with the fraction of molecular hydro-

**Table 2.** Equivalent widths (from literature and archival data) and calculated column densities of OH and CH transitions

Source	$E_{B-V}$	EW(3078)	EW(3082)	EW(3137)	EW(3143)	EW(3886)	EW(3890)	$N(\text{OH})$	$N(\text{CH})$	$N(\text{CH})$
		m	m	m	m	m	m	$\text{cm}^{-2}$	(3137+3143) $\text{cm}^{-2}$	(3886+3890) $\text{cm}^{-2}$
HD24398 <sup>1</sup>	0.29	1.67±0.08	1.11±0.05	3.25±0.41	5.83±0.36	4.96±0.50	3.01±0.38	3.93±0.18(13)	2.84±0.29(13)	2.23±0.25(13)
HD27778 <sup>1,3</sup>	0.37	5.30±0.15	2.20±0.10	3.15±1.08	9.2±1.0	7.46±0.60	4.84±0.80	1.01±0.04(14)	3.366±0.77(13)	3.99±0.41(13)
HD34078 <sup>1</sup>	0.49	1.72±0.27	0.86±0.21	6.92±1.36	19.9±1.4	16.75±1.30	11.28±0.50	3.53±0.69(13)	7.34±0.99(13)	7.93±0.48(13)
BD-14 5037 <sup>a,2</sup>	1.59	5.74±0.43	5.71±0.60	3.2±0.21	10.64±0.33	9.47±0.5	6.15±0.5	1.70±0.16(14)	3.65±0.17(13)	4.40±0.22(13)
HD110432 <sup>1</sup>	0.48	1.81±0.41	1.28±0.34	1.83±0.28	5.14±0.38	4.13±0.20	2.40±0.20	4.41±1.09(13)	1.92±0.22(13)	1.82±0.12(13)
HD114213 <sup>b</sup>	1.13	9.86±0.96	8.30±0.87	4.48±0.27	10.64±0.42	...	...	2.64±0.27(14)	4.35±0.22(13)	...
HD147889	1.08	12.19±0.45	5.38±0.20	10.8±0.24	22.48±0.20	20.07±1.20	15.02±0.98	2.37±0.09(14)	9.92±0.17(13)	1.00±0.06(14)
HD147933 <sup>2</sup>	0.48	3.63±0.27	2.02±0.31	3.14±0.28	5.69±0.12	5.68±0.35	3.46±0.26	7.83±0.88(13)	2.73±0.17(13)	2.56±0.17(13)
HD148688 <sup>1</sup>	0.55	0.92±0.45	0.81±0.54	1.54±0.22	4.28±0.28	3.83±0.20	2.75±0.20	2.53±1.50(13)	1.61±0.17(13)	1.87±0.12(13)
HD149757	0.28	2.01±0.67	1.25±0.32	3.54±0.30	6.52±0.17	5.45±0.20	3.57±0.10	4.58±1.35(13)	3.10±0.19(13)	2.54±0.08(13)
HD151932 <sup>1</sup>	0.50	4.46±0.71	2.13±0.54	2.68±0.12	7.04±0.47	5.97±0.78	3.60±0.10	8.97±1.80(13)	2.72±0.15(13)	2.68±0.22(13)
HD152236	0.66	3.50±0.44	2.41±0.34	...	...	5.34±0.45	4.15±0.56	8.40±1.12(13)	...	2.72±0.30(13)
HD152249	0.48	2.81±1.00	1.82±0.80	...	...	3.40±0.50	2.61±0.40	6.53±2.60(13)	...	1.72±0.26(13)
HD152270	0.50	1.95±0.64	2.13±0.70	...	...	3.52±0.43	2.69±0.45	6.12±2.01(13)	...	1.78±0.26(13)
HD154368	0.47	9.25±0.58	4.01±0.31	5.73±0.26	14.79±0.24	12.24±1.10	9.32±0.40	1.79±0.12(14)	5.78±0.19(13)	6.18±0.40(13)
HD154445 <sup>1,3</sup>	0.35	2.01±0.31	1.52±0.33	2.43±0.51	6.50±0.29	4.35±0.50	3.76±0.65	5.07±0.96(13)	2.49±0.33(13)	1.96±0.12(13)
HD154811	0.66	2.43±0.70	1.64±0.50	...	...	5.03±0.34	3.12±0.56	5.77±1.71(13)	...	2.29±0.28(13)
HD161056 <sup>2</sup>	0.59	10.71±0.61	6.78±0.50	5.63±0.30	14.23±0.45	10.3±0.8	9.5±0.55	2.46±0.16(14)	5.62±0.24(13)	5.79±0.38(13)
HD163800	0.61	2.00±0.17	1.85±0.12	3.42±0.15	7.97±0.09	6.85±0.30	5.16±0.40	5.67±0.41(13)	3.29±0.10(13)	3.44±0.21(13)
HD164794	0.36	1.55±0.40	1.00±0.65	...	...	2.29±0.54	1.83±0.34	3.59±1.65(13)	...	1.19±0.25(13)
HD169454	1.10	6.24±0.25	2.90±0.22	4.52±0.27	11.01±0.30	8.51±0.54	6.47±0.43	1.24±0.07(14)	4.44±0.20(13)	4.29±0.28(13)
HD170740	0.45	1.97±0.43	1.73±0.31	2.16±0.16	6.56±0.22	5.10±0.29	2.84±0.20	5.41±1.06(13)	2.35±0.13(13)	2.20±0.14(13)
HD172028	0.79	5.05±0.50	4.09±0.35	5.81±0.35	15.59±0.30	...	...	1.32±0.12(14)	5.96±0.24(13)	...
HD210121 <sup>2</sup>	0.40	4.45±0.28	3.03±0.23	3.31±0.24	8.31±0.19	6.51±0.31	5.83±0.50	1.06±0.07(14)	3.29±0.17(13)	3.59±0.25(13)

<sup>a</sup> BD-14 5037 shows absorptions at two velocities around  $-5 \text{ km s}^{-1}$  and  $6 \text{ km s}^{-1}$ . Since only  $-5 \text{ km s}^{-1}$  component is seen in the OH(3081) spectral line, the numbers correspond to this component.

<sup>b</sup> HD 114213 shows absorptions at two velocities around  $-20 \text{ km s}^{-1}$  and  $6 \text{ km s}^{-1}$  for CH and  $-20 \text{ km s}^{-1}$  and  $3 \text{ km s}^{-1}$  for OH. We present here the  $-20 \text{ km s}^{-1}$ , which is uniquely identified in all the spectral lines considered here.

<sup>1</sup> Sources for which we measured EW(3137) and EW(3143).

<sup>2</sup> Sources for which we measured EW(3886) and EW(3890).

<sup>3</sup> Sources for which we derived EW(3886) and EW(3890) slightly different from the published values.

gen in these clouds. We show that except for the line of sight toward HD 34078 which is thought to show signatures of shock-induced increase in CH abundance, the observed OH/CH ratios in all other clouds are well reproduced by the chemical models considered here.

## ACKNOWLEDGEMENTS

BM sincerely thanks the referee Jacek Krelowski for suggestions which enhanced the scope of the paper by including additional data. BM thanks J. P. Ninan for his help with many python related issues. This research has made use of the VizieR catalogue access tool, CDS, Strasbourg, France. The original description of the VizieR service was published in A&AS 143, 23.

## REFERENCES

Bhatt N. H., Cami J., 2015, ApJS, 216, 22  
 Bohlin R. C., Savage B. D., Drake J. F., 1978, ApJ, 224, 132  
 Boissé P., et al., 2009, A&A, 501, 221  
 Boissé P., Le Petit F., Rollinde E., Roueff E., Pineau des Forêts G., Andersson B.-G., Gry C., Felenbok P., 2005, A&A, 429, 509  
 Chaffee F. H., Jr., Lutz B. L., 1977, ApJ, 213, 394

Crutcher R. M., Watson W. D., 1976, ApJ, 203, L123  
 Federman S. R., 1982, ApJ, 257, 125  
 Felenbok P., Roueff E., 1996, ApJ, 465, L57  
 Herbig G. H., 1968, ZA, 68, 243  
 Krelowski J., Ehrenfreund P., Foing B. H., Snow T. P., Weselak T., Tuairisg S. Ó., Galazutdinov G. A., Musaev F. A., 1999, A&A, 347, 235  
 Lien D. J., 1984, ApJ, 284, 578  
 Maret S., Bergin E. A., 2015, ascl.soft, ascl:1507.010  
 Mattila K., 1986, A&A, 160, 157  
 Roueff E., 1996, MNRAS, 279, L37  
 Sheffer Y., Rogers M., Federman S. R., Abel N. P., Gredel R., Lambert D. L., Shaw G., 2008, ApJ, 687, 1075  
 Wagenblast R., Williams D. A., Millar T. J., Nejad L. A. M., 1993, MNRAS, 260, 420  
 Weinreb S., Barrett A. H., Meeks M. L., Henry J. C., 1963, Natur, 200, 829  
 Weselak T., Galazutdinov G. A., Beletsky Y., Krelowski J., 2010, MNRAS, 402, 1991  
 Weselak T., Galazutdinov G., Beletsky Y., Krelowski J., 2009, A&A, 499, 783  
 Weselak T., Galazutdinov G. A., Musaev F. A., Krelowski J., 2004, A&A, 414, 949  
 Wiesemeyer H., et al., 2016, A&A, 585, A76

This paper has been typeset from a  $\text{\TeX}/\text{\LaTeX}$  file prepared by the author.

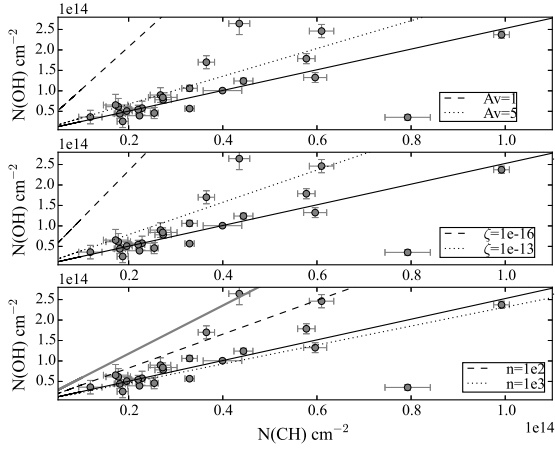


**Figure 4.** Comparison of observed column densities of OH and CH with computed values from the chemical model Astrochem (Maret & Bergin 2015) used with the chemical network OSU2009. The solid black line in all panels represents Model A with  $n_{\text{H}}=500 \text{ cm}^{-3}$ ,  $\zeta_{\text{CR}} = 10^{-14} \text{ s}^{-1}$ ,  $A_{\text{V}}=2.0$ ,  $f_{\text{H}_2}=0.3$ ,  $\chi = 5$  and  $T_{\text{gas}}=30 \text{ K}$ . *Top left:* Model A with  $A_{\text{V}}=1$  (dashed) and  $A_{\text{V}}=5$  (dotted); *Top Right:* Model A with  $\zeta_{\text{CR}} = 10^{-16} \text{ s}^{-1}$  (dashed) and  $\zeta_{\text{CR}} = 10^{-13} \text{ s}^{-1}$  (dotted); *Bottom Left:* Model A with  $n_{\text{H}} = 100 \text{ cm}^{-3}$  (dashed) and  $n_{\text{H}} = 1000 \text{ cm}^{-3}$  (dotted). The thick grey line shows the trace of the model ( $n_{\text{H}}=500 \text{ cm}^{-3}$ ,  $\zeta_{\text{CR}} = 2.5 \cdot 10^{-16} \text{ s}^{-1}$ ,  $A_{\text{V}}=3.0$ ,  $f_{\text{H}_2}=0.3$ ,  $\chi = 1$  and  $T_{\text{gas}}=30 \text{ K}$ ), which explains the OH/CH ratio of HD 114213.